A Novel Computational Method for Panel Acoustic Contribution Analysis in a Cabin Based on Helmholtz Equation Least Squares

Yue Xiao[1], Mouyou Lin[1] and Zhenxi Wang[2]

[1]*Jiangxi Province Key Laboratory of Precision Drive and Control, School of Mechanical and Electrical Engineering, Nanchang Institute of Technology, Nanchang 330099, China*
[2]*School of Science, Nanchang Institute of Technology, Nanchang 330099, China*
popxy90@163.com, lmyst2000@163.com, wangzhenxi1978@126.com

Abstract

Panel acoustic contribution analysis (PACA) is an advanced engineering tool for noise control and acoustic design in a cabin. In this study, a novel computational method for PACA by using Helmholtz equation least squares (HELS) based on nearfield acoustical holography (NAH) was proposed. According to the new very definition of panel acoustic contribution, formulations of the present method are derived to analyze the relative panel acoustic contributions of each panel in the interior sound field. The significance of this methodology is that it can provide either positive or negative contribution and rank relative acoustic contributions of individual panels to acoustic radiation anywhere in the field based on a single set of the acoustic pressures measured in the near field. A numerical simulation of a scaled vehicle cabin has been investigated to demonstrate the validity of this method. Moreover, the results show the advantage of the proposed method, since it could reflect the contributions of individual panels more correctly than the ranking of acoustic power.

Keywords: Panel acoustic contribution analysis, Helmholtz equation least squares method; nearfield acoustical holography

1. Introduction

In engineering, the interior sound field inside an elastic cavity is the most representative, such as the passenger compartments of automobiles, ships and airplanes [1]. A major factor affecting the interior sound field is the vibrational and acoustic behavior of all the panels around it. Panel acoustic contribution analysis has been developed to determine the relative contributions of individual panels at a certain listening position in the interior sound field, and pinpoint the local areas of the panel that need modification [2-4]. It plays an important role to improve noise, vibration, and harshness quality, and is of great significance for the noise control and acoustic design. Currently, the experimental and numerical methods are mostly used to identify the acoustic contribution of panel. The experimental methods mainly include masking/window method, transfer path analysis (TPA) method [5, 6] and reciprocity measurement method [7, 8], *etc*. The masking technique is high costs, and the changes of acoustic environment in the interior sound field and the vibration of the structure surface will affect the identification accuracy. For TPA and reciprocity measurement method, the enormous works are needed to measure the vibration strength and to establish the transfer function between an excitation and a response, and the result is effective only in the position of measurement point. The finite element method (FEM) [9] and the boundary element method (BEM) [10], both of which belong to the numerical methods, can be applied to any shaped structure or cavity but with huge computational cost, and the analysis

accuracy depends largely on the simplified rationality of the model and boundary conditions.

In recent years, nearfield acoustical holography has proven to be a powerful tool for identifying noise source and predicting sound field [11-14]. Xiao *et al.* [15] employed NAH based on the equivalent source method (ESM) to identify the relative contributions of individual panels in irregular enclosed sound field. Wu *et al.* [16, 17] proposed the Helmholtz equation least squares (HELS) based NAH to analyze relative acoustic contributions from vibrating structures. In his work, the sound pressure level at a field point was correlated to the acoustic power flow from each panel, and thus by only measuring a set of holographic sound pressure, the contributions of individual panels to the sound pressure level (SPL) at any field point could be ranked. According to Wu, the SPL value at the specific field point and the net acoustic power from this panel were defined as the panel acoustic contribution respectively. However, the SPL value cannot be used to rank relative acoustic contributions since it is invariably positive. Meanwhile, the net acoustic power cannot reflect the information for the specified point in the field, although it can provide either negative or positive values. Considering the above situation, the net acoustic power is always used rather than the SPL calculation to estimate and rank the relative acoustic contributions. Therefore, the use of panel acoustic contribution defined by the algorithm may have less function in engineering practice, and is not completely suitable for interior sound field refinement.

In order to improve on the present PACA method, this paper introduces a novel computational approach based on HELS by using the theory of interior nearfield acoustic holography. The method was formulated to the very definition of contribution, thus the calculated contributions would be either positive or negative, and totally dependent with the position of the field point. The presented method will inherit all the advantages of the HELS. Furthermore, it can give a more deep insight to the contribution of each panel. The methodology helps to determine the optimum locations and to provide guidelines for structure modifications according to the acoustic contributions of each panel to the interior sound field.

2. Theoretical Background

2.1. Interior NAH based on HELS

HELS is an effective method to compute both the interior [18] and exterior [19] NAH problems, it uses an expansion of the spherical wave functions to approximate the real sound field. For the interior problems such as inside a cavity, the sound field can be presented by a series of spherical harmonic expansions. As shown in Figure 1, the sound pressure and particle velocity at a field point in the spherical coordinate system can be expressed as

$$p(\boldsymbol{r}) \approx \sum_{n=0}^{N} \sum_{m=-n}^{n} C_{mn} j_n(kr) Y_n^m(\theta,\varphi) = \sum_{j=1}^{J} C_j \psi_{p,j}(\boldsymbol{r}) \tag{1}$$

where N is the cutoff order of spherical harmonics, $j = n^2 + n + m + 1$, $J = (N+1)^2$, $C_j = C_{mn}$ is the spherical expansion coefficient, $\psi_{p,j} = \psi_{p,mn} = j_n(kr) Y_n^m(\theta,\varphi)$ is the expansion function, $j_n(kr)$ is the Bessel function of the first kind which is bounded at $\boldsymbol{r} = 0$, and $Y_n^m(\theta,\varphi)$ is spherical harmonics function. Here,

$$Y_n^m(\theta,\varphi) = \sqrt{\frac{(2n+1)}{4\pi}\frac{(n-m)!}{(n+m)!}} P_n^m(\cos\theta) e^{im\varphi} \tag{2}$$

Given M measurement points on the hologram, the measured pressure can be written in a matrix form as,

$$P_h = \Psi_{ph} C \tag{3}$$

in which

$$P_h = [p(r_{h,1}), p(r_{h,2}), \cdots, p(r_{h,M})]^T \tag{4}$$

$$\Psi_{ph} = \begin{bmatrix} \psi_{p,1}(r_{h,1}) & \psi_{p,2}(r_{h,1}) & \cdots & \psi_{p,J}(r_{h,1}) \\ \psi_{p,1}(r_{h,2}) & \psi_{p,2}(r_{h,2}) & \cdots & \psi_{p,J}(r_{h,2}) \\ \vdots & \vdots & \ddots & \vdots \\ \psi_{p,1}(r_{h,M}) & \psi_{p,2}(r_{h,M}) & \cdots & \psi_{p,J}(r_{h,M}) \end{bmatrix} \tag{5}$$

$$C = [C_1, C_2, \cdots, C_J]^T \tag{6}$$

where P_h is sound pressure column vector on any measurement surface, the superscript "T"' denotes the matrix transpose, $r_{h,m}$ represent is the location vector of the m-th measurement point on the hologram surface, Ψ_{ph} is the spherical wave source matrix of holographic sound pressure, and C is the weight coefficient column vector.

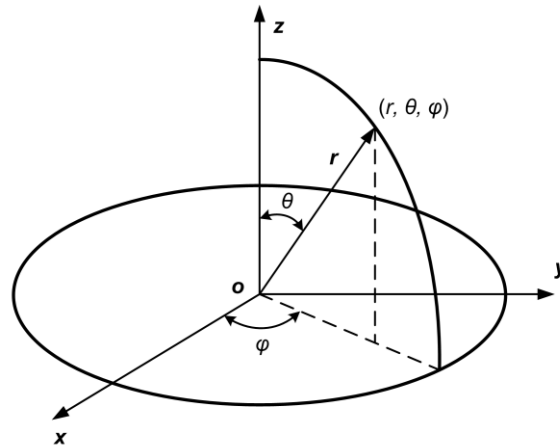**Figure 1. Definition of Spherical Coordinates**

By inversion of Eq. (3), the weight coefficient column vector can be obtained

$$C = (\Psi_{ph})^+ P_h \tag{7}$$

where "+" denotes the general inverse. In practical calculation, $(\Psi_{ph})^+$ is obtained by singular value decomposition. To restrict the influence of the input error on the reconstructed results, the regularization method is required to stabilize the solution procedure, since there will inevitably be noises in the actual hologram measurement.

By using the weight coefficient column vector C, the sound pressure in the cavity can be expressed as

$$p_{fp} = \Psi_p C \tag{8}$$

where p_{fp} is the sound pressure at a concerned field point in the cavity, $\Psi_p = [\psi_{p,1}(r_{fp}), \psi_{p,2}(r_{fp}), \cdots, \psi_{p,J}(r_{fp})]$ is the spherical wave source matrix of reconstructed sound pressure.

Similarly, suppose that there are S reconstructed points on the surface of the cavity, the normal surface velocity can also be expressed with a set of spherical expansions as

$$V_s = \Psi_{vs} C \tag{9}$$

where V_s is the column vector of the normal surface velocity on the surface of the cavity. $\boldsymbol{\Psi}_{vs}$ is the spherical wave source matrix of reconstructed normal surface velocity through Euler's equation. Here,

$$\boldsymbol{\Psi}_{vs} = \frac{1}{i\rho ck} \begin{bmatrix} \dfrac{\partial\psi_{p,1}(\boldsymbol{r}_{s,1})}{\partial n} & \dfrac{\partial\psi_{p,2}(\boldsymbol{r}_{s,1})}{\partial n} & \cdots & \dfrac{\partial\psi_{p,J}(\boldsymbol{r}_{s,1})}{\partial n} \\ \dfrac{\partial\psi_{p,1}(\boldsymbol{r}_{s,2})}{\partial n} & \dfrac{\partial\psi_{p,2}(\boldsymbol{r}_{s,2})}{\partial n} & \cdots & \dfrac{\partial\psi_{p,J}(\boldsymbol{r}_{s,2})}{\partial n} \\ \vdots & \vdots & \ddots & \vdots \\ \dfrac{\partial\psi_{p,1}(\boldsymbol{r}_{s,S})}{\partial n} & \dfrac{\partial\psi_{p,2}(\boldsymbol{r}_{s,2})}{\partial n} & \cdots & \dfrac{\partial\psi_{p,J}(\boldsymbol{r}_{s,S})}{\partial n} \end{bmatrix} \tag{10}$$

where ρ is the density of the medium, c is the speed of sound, $k = \omega/c$ is the wave number, and ω is the angular frequency.

Combining Eq. (7) and Eq. (9), the normal surface velocity on the surface of the cavity can be obtained as

$$V_s = \boldsymbol{\Psi}_{vs}(\boldsymbol{\Psi}_p)^+ \boldsymbol{P}_h \tag{11}$$

2.2 Formulation for Acoustic Contribution Analysis

Assuming the entire surface of the cavity is composed of K panels, the sound pressure p_{fp} at the concerned field point can be considered as the superposition of the sound pressures produced by all of the vibrating panels, and this relationship can be described as

$$p_{fp} = \sum_{k=1}^{K} p_k \tag{12}$$

where p_k is the sound pressure produced by the k-th panel at the concerned field point, $k = 1, \cdots, K$.

By using Eq. (8), the sound pressure produced by the k-th panel at the concerned field point can be expressed as

$$p_k = \boldsymbol{\Psi}_p \boldsymbol{C}_k \tag{13}$$

where C_k is the weight coefficient column vector corresponding to the k-th panel.

For the enclosed sound field formed by all of the vibrating panels of the cavity, by using Eq. (9), the weight coefficient column vector can be obtained as

$$\boldsymbol{C} = (\boldsymbol{\Psi}_{vs})^+ \boldsymbol{V}_s \tag{14}$$

Obviously, the column vector of the normal surface velocity V_s can be written as

$$\boldsymbol{V}_s = [\boldsymbol{V}_{s1}^{\mathrm{T}}, \cdots, \boldsymbol{V}_{sk}^{\mathrm{T}}, \cdots, \boldsymbol{V}_{sK}^{\mathrm{T}}]^{\mathrm{T}} \tag{15}$$

where V_{sk} is the column vector of the normal velocity corresponding to the k-th panel.

Thus Eq. (14) can be written as

$$\boldsymbol{C} = (\boldsymbol{\Psi}_{vs})^+ [\boldsymbol{V}_{s1}^{\mathrm{T}}, \cdots, \boldsymbol{V}_{sk}^{\mathrm{T}}, \cdots, \boldsymbol{V}_{sK}^{\mathrm{T}}]^{\mathrm{T}} \tag{16}$$

According to the physical meaning of the panel acoustic contribution, it is obviously seen that for calculating the sound pressure produced by the k-th panel at the specific field point, only the normal surface velocity on the k-th panel is reserved, while the others are set to zeros. From Eq. (16), the weight coefficient column vector corresponding to the k-th panel can be obtained as

$$\boldsymbol{C}_k = (\boldsymbol{\Psi}_{vs})^+ [\boldsymbol{O}, \cdots, \boldsymbol{V}_{sk}^{\mathrm{T}}, \cdots, \boldsymbol{O}]^{\mathrm{T}} \tag{17}$$

Substituting Eq. (17) into the right side of Eq. (13), it can be obtained as

$$p_k = \boldsymbol{\Psi}_p (\boldsymbol{\Psi}_{vs})^+ [\boldsymbol{O}, \cdots, \boldsymbol{V}_{sk}^{\mathrm{T}}, \cdots, \boldsymbol{O}]^{\mathrm{T}} \tag{18}$$

Equation (18) shows that the sound pressure produced by the k-th panel at the concerned field point may be correlated to the normal velocity corresponding to the k-th panel.

Suppose that there are P_k points on the k-th panel and the order of those points is $r_{k,1}$, , $r_{k,2}$,…, r_{k,P_k} in turn, which satisfies $\sum_{k=1}^{K} P_k = S$ .By using Eq. (10), $\boldsymbol{\Psi}_{vs}$ can be written in a matrix form as

$$\boldsymbol{\Psi}_{vs} = \frac{1}{\mathrm{i}\rho ck} \begin{bmatrix} \dfrac{\partial \psi_{p,1}(\boldsymbol{r}_{s,1})}{\partial n} & \dfrac{\partial \psi_{p,2}(\boldsymbol{r}_{s,1})}{\partial n} & \cdots & \dfrac{\partial \psi_{p,J}(\boldsymbol{r}_{s,1})}{\partial n} \\ \dfrac{\partial \psi_{p,1}(\boldsymbol{r}_{s,2})}{\partial n} & \dfrac{\partial \psi_{p,2}(\boldsymbol{r}_{s,2})}{\partial n} & \cdots & \dfrac{\partial \psi_{p,J}(\boldsymbol{r}_{s,2})}{\partial n} \\ \vdots & \vdots & \ddots & \vdots \\ \dfrac{\partial \psi_{p,1}(\boldsymbol{r}_{s,S})}{\partial n} & \dfrac{\partial \psi_{p,2}(\boldsymbol{r}_{s,2})}{\partial n} & \cdots & \dfrac{\partial \psi_{p,J}(\boldsymbol{r}_{s,S})}{\partial n} \end{bmatrix} = \begin{bmatrix} \boldsymbol{\Psi}_{sv1} \\ \vdots \\ \boldsymbol{\Psi}_{svk} \\ \vdots \\ \boldsymbol{\Psi}_{svK} \end{bmatrix} \quad (19)$$

Thus $\boldsymbol{\Psi}_{svk}$ can be expressed as

$$\boldsymbol{\Psi}_{svk} = \frac{1}{\mathrm{i}\rho ck} \begin{bmatrix} \dfrac{\partial \psi_{p,1}(\boldsymbol{r}_{k,1})}{\partial n} & \dfrac{\partial \psi_{p,2}(\boldsymbol{r}_{k,1})}{\partial n} & \cdots & \dfrac{\partial \psi_{p,J}(\boldsymbol{r}_{k,1})}{\partial n} \\ \dfrac{\partial \psi_{p,1}(\boldsymbol{r}_{k,2})}{\partial n} & \dfrac{\partial \psi_{p,2}(\boldsymbol{r}_{k,2})}{\partial n} & \cdots & \dfrac{\partial \psi_{p,J}(\boldsymbol{r}_{k,2})}{\partial n} \\ \vdots & \vdots & \ddots & \vdots \\ \dfrac{\partial \psi_{p,1}(\boldsymbol{r}_{k,P_k})}{\partial n} & \dfrac{\partial \psi_{p,2}(\boldsymbol{r}_{k,P_k})}{\partial n} & \cdots & \dfrac{\partial \psi_{p,J}(\boldsymbol{r}_{k,P_k})}{\partial n} \end{bmatrix} \quad (20)$$

Combining Eq. (11), Eq. (15) and Eq. (19), it can be obtained as

$$[\boldsymbol{O},\cdots,\boldsymbol{V}_{sk}^{\mathrm{T}},\cdots,\boldsymbol{O}]^{\mathrm{T}} = [\boldsymbol{O},\cdots,\boldsymbol{\Psi}_{svk}^{\mathrm{T}},\cdots,\boldsymbol{O}]^{\mathrm{T}} (\boldsymbol{\Psi}_p)^+ \boldsymbol{P}_h \quad (21)$$

Substituting Eq. (21) into the right side of Eq. (18), the sound pressure produced by the k-th panel at the concerned field point can be expressed as

$$p_k = \boldsymbol{\Psi}_p (\boldsymbol{\Psi}_{vs})^+ [\boldsymbol{O},\cdots,\boldsymbol{\Psi}_{svk}^{\mathrm{T}},\cdots,\boldsymbol{O}]^{\mathrm{T}} (\boldsymbol{\Psi}_p)^+ \boldsymbol{P}_h \quad (22)$$

Note that Eq. (22) is valid for any position of field points based on a single set of input data of hologram measurement. In other words, panel acoustic contribution analysis can be repeated again and again without the need to retake input data, thus significantly enhancing the efficiency in acoustic contribution analyses.

Once the sound pressure produced by the k-th panel at the concerned field point has been obtained, the normalized acoustic contribution of this panel to the specified point anywhere in the field can be calculated as

$$D_k = \mathrm{Re}(\frac{p_k \cdot p_{fp}^*}{\left| p_{fp} \right|^2}) \quad (23)$$

where D_k is the acoustic contribution of the k-th panel, "Re" indicates the real part, and the superscript " $*$ " indicates the complex conjugate operator.

According to the definition of panel acoustic contribution, the contribution can be either positive or negative. If the contribution of a panel is positive, it means the sound pressure produced by the panel is in-phase with respect to the total sound pressure at the concerned field point, thus the total sound pressure increases as the normal surface velocity of the panel increases, whereas a negative contribution indicate the total sound pressure decreases as the normal surface velocity of the panel increases.

It should be mentioned that for a surface with acoustic treatments, the normal velocity in the above should be replaced by the surface pressure divided by surface acoustic impedance.

3. Numerical Validation

A scaled car cabin model was used to test the proposed method. The cabin was composed of seven panels and the material of the panels was steel, with the density of 7.8×10^3 kg/m^3, the Young's modulus was 210 GPa, and the Poisson ratio was 0.3.The dimension of the cabin was shown in Figure 2, the thickness of the panels was 2 mm. The bottom panel was excited with a point force of 0.2 N at (0.388 m, 0.235 m, 0), over the frequency range of 20 ~ 250 Hz. The measurement of pressure was made 2.5 cm away from the interior surface of the cabin, and a total of 721 points was measured. The field point located at (0.3 m, 0.3 m, 0.3 m) was chosen as the observation point.
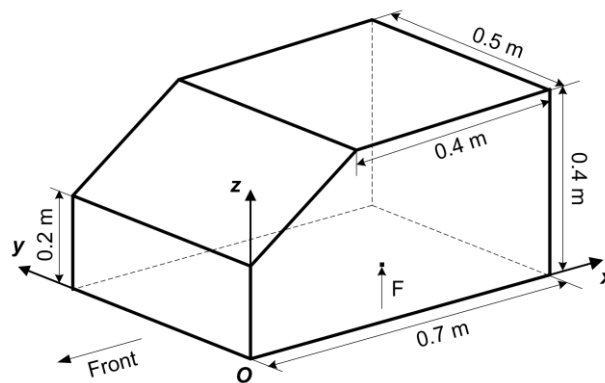

Figure 2. Sketch of Scaled Cabin

Due to the difficulty of describing the irregular interior sound field with analytic expression, the finite element method (FEM) for acoustics in LMS Virtual. Lab was adopted to calculate the theoretical sound pressures on the hologram surface and at the observation point. In addition, the sound pressures on the hologram were used as input data for the interior NAH reconstruction. In order to simulate the practical measurement, a Gauss noise has been added to the measured data corresponding to a signal-to-noise ratio of 30 dB. Based on the "measured" pressures on the hologram surface, the proposed method can be used to predict the sound field and to rank the acoustic contribution of each panel.

Firstly, the pressure at the observation point should be reconstructed. Figure 3 shows comparison of the reconstructed and the theoretical sound pressure at the observation point in dB over the whole frequency range. It can be seen that the reconstructed sound pressure agreed almost perfectly with the theoretical values.
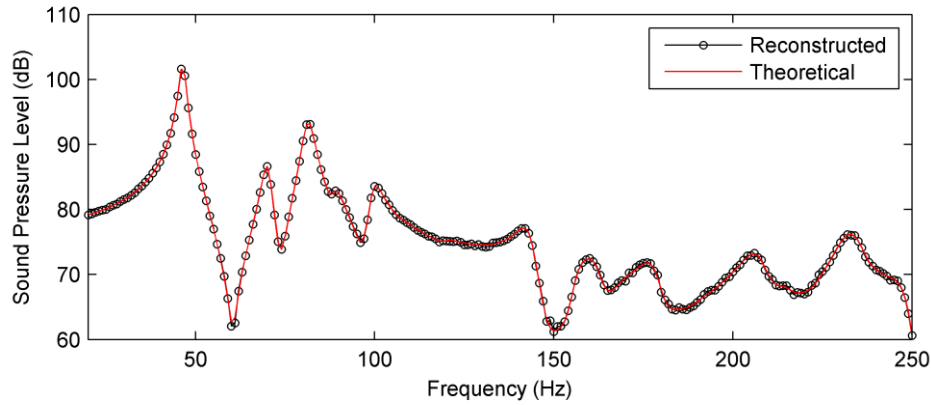
Figure 3. Comparison of the Reconstructed Sound Pressure (dB ref. 20μPa) and the Theoretical Value at the Observation Point.

The next step for analysis of panel acoustic contribution is to determine the frequencies that correspond to the peak values of the Sound Pressure Level (SPL). The frequencies corresponding to the first two peak responses were 46 Hz and 82 Hz, as shown in Figure 3. Thus the panel acoustic contribution analysis will be implemented at these frequencies.
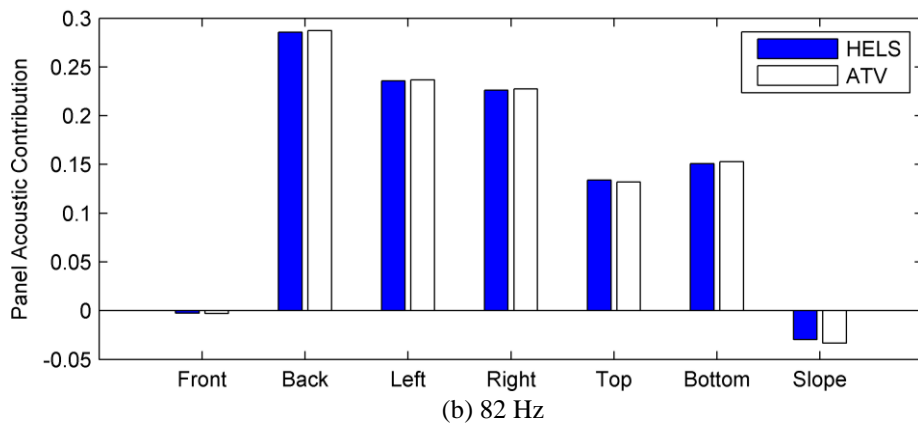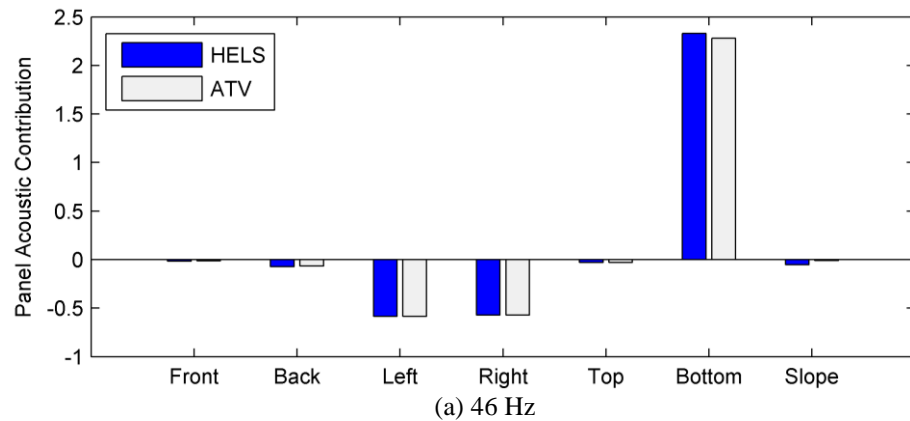

(a) 46 Hz

(b) 82 Hz

Figure 4. Comparisons of the Panel Acoustic Contributions in the Proposed Method and in ATV Method

As a comparison, the acoustic transfer vector (ATV) method which is integrated in the LMS Virtual. Lab is used to serve as the reference. Figure 4 shows the comparisons of the

panel acoustic contributions in the proposed method and in ATV method at 46 Hz and 82 Hz. It can be seen that good agreements were obtained for all panels, which demonstrate the ability of ranking the panel acoustic contributions. It also can be found that the panel acoustic contributions to the sound field will vary for different panels at the different frequencies. Note that there are both positive and negative values of the panel acoustic contributions, of which the former indicates the sound pressure at the specified field point increases as the normal velocities on the panel increase, and the latter indicates the exact opposite of the former. In the noise control, it is recommended that one should take measures to reduce vibration of the panel with greater positive contribution, while utilize vibration of the panel with greater negative contribution to attenuate the pressure at the specified field point.

The ranking with the relative contributions from all panels based on the acoustic power is also shown in Figure 5. Although the ranking could reflect the quantity that contributed by each panel, it cannot provide a correct positive or negative property of the contributions. This is because the acoustic power is not correlated to a specified field point but give an overall reflection. Take the left and the right panels for example, the left panel gives almost the same contribution as the right panel, while the signs of the acoustic powers are opposite since the directions of the velocities on the two panels are opposite. However, when the velocities are correlated to the sound pressure at the observation point, both the panels give positive contributions, and this is not reflected from the ranking of acoustic power.
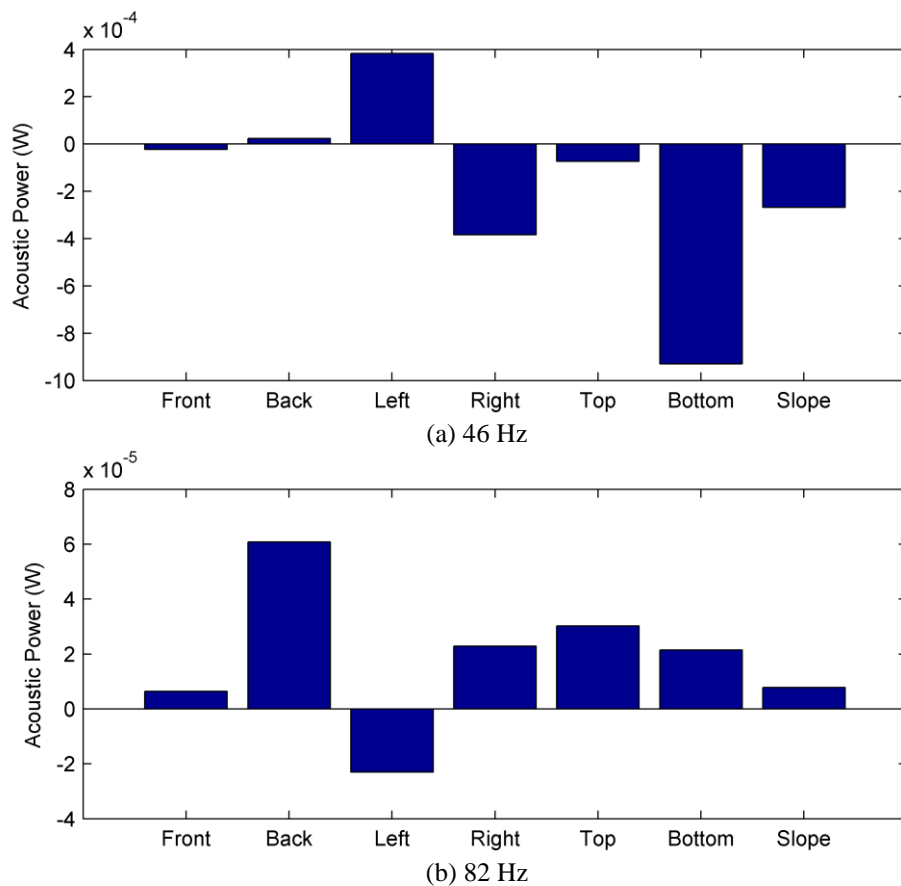

(a) 46 Hz

(b) 82 Hz

Figure 5. Relative Contributions from All Panels Based on the Acoustic Power

According to the comparison above, it is found that the proposed method can more correctly reflect the contributions of individual panels than the ranking of acoustic power, since the latter does not correlate the panels to a specific field point.

4. Conclusion

The shortcomings of the current PACA approach have been improved by using a novel computational method of panel contribution. A modified HELS based NAH method for panel acoustic contribution is proposed, and the validity of the method was testified with a numerical simulation. The method was formulated from the very definition of contribution, thus can yield either positive or negative contribution. Compared to the ranking of acoustic power, the method can more correctly reflect the contributions of individual panels than the ranking of acoustic power since the acoustic power only gives overall information of contribution. In particular, it enables one to rank relative contributions from individual panels of an arbitrarily shaped structure to the resultant acoustic field based on a single set of the acoustic pressure measurements.

Acknowledgements

References

[1] W. Ding and H. Chen, "Research on the interior noise contributed from a local panel's vibration of an elastic thin-walled cavity", Applied Acoustics, vol. 63, no. 1, **(2002)**, pp. 95-102.

[2] S. Marburg, H. -J. Beer, J. Gier, H. -J. Hardtke, R. Rennert and F. Perret, "Experimental verification of structural-acoustic modeling and design optimization", Journal of Sound and Vibration, vol. 252, no. 4, **(2002)**, pp. 591-615.

[3] O. Wolff, "Fast panel noise contribution analysis using large PU sensor arrays", Proceedings of Inter-Noise, Istanbul, Turkey, **(2007)**, pp. 1112-1121.

[4] X. Han, Y. -J. Guo, H. -D. Yu and P. Zhu, "Interior sound field refinement of a passenger car via modified panel acoustic contribution analysis", International Journal of Automotive Technology, vol. 10, no. 1, **(2009)**, pp. 79-85.

[5] J. Plunt, "Finding and fixing vehicle NVH problems with transfer path analysis", Sound and Vibration, vol. 39, no. 11, **(2005)**, pp. 12-17.

[6] A. N. Thite and D. J. Thompson, "The quantification of structure-borne transmission paths by inverse methods. Part 2: Use of regularization techniques", Journal of Sound and Vibration, vol. 264, no. 2, **(2003)**, pp. 433-451.

[7] J. W. Verheij, "Inverse and Reciprocity Methods for Machinery Noise Source Characterization and Sound Path Quantification", International Journal of Acoustics and Vibration, vol. 2, no. 1, **(1997)**, pp. 11-20.

[8] F. J. Fahy, "Some Applications of the Reciprocity Principle in Experimental Vibroacoustics", Acoustical Physics, vol. 49, no. 2, **(2003)**, pp. 217-229.

[9] C. L. Teik, "Automotive panel noise contribution modeling based on finite element and measured structural-acoustic spectra", Applied Acoustics, vol. 60, no. 4, **(2000)**, pp. 505-519.

[10] B. K. Kim and J. G. Ih, "On the reconstruction of the vibro-acoustic field over the surface enclosing an interior space using the boundary element method", Journal of the Acoustical Society of America, vol. 100, no. 5, **(1996)**, pp. 3003-3016.

[11] J. D. Maynard, E. G. Williams and Y. Lee, "Nearfield acoustic holography: I. Theory of generalized holography and the development of NAH", Journal of the Acoustical Society of America, vol. 78, no. 4, **(1985)**, pp. 1395-1413.

[12] E. G. Williams and B. H. Houston, "Interior near-field acoustical holography in flight", Journal of the Acoustical Society of America, vol. 108, no. 4, **(2000)**, pp. 1451-1463.

[13] S. F. Wu and X. Zhao, "Combined Helmholtz equation–least squares method for reconstructing acoustic radiation from arbitrarily shaped objects", Journal of the Acoustical Society of America, vol. 112, no. 1, **(2002)**, pp. 179-188.

[14] S. F. Wu, "Methods for reconstructing acoustic quantities based on acoustic pressure measurements", Journal of the Acoustical Society of America, vol. 124, no. 5, **(2008)**, pp. 2680-2697.

[15] Y. Xiao, J. Chen and D. Y. Hu, "Equivalent source method for identification of panel acoustic contribution in irregular enclosed sound field", Chinese Journal of Acoustics, vol. 34, no. 1, **(2015)**, pp. 49-66.

[16] S. F. Wu and L. K. Natarajan, "Panel acoustic contribution analysis", Journal of the Acoustical Society of America, vol. 133, no. 2, **(2013)**, pp. 799-809.

[17] S. F. Wu, M. Moondra and R. Beniwal, "Analyzing panel acoustic contributions toward the sound field inside the passenger compartment of a full-size automobile", Journal of the Acoustical Society of America, vol. 137, no. 4, **(2015)**, pp. 2101-2112.

[18] S. F. Wu and J. Yu, "Reconstructing interior acoustic pressure field via Helmholtz equation least-squares method", Journal of the Acoustical Society of America, vol. 104, no. 4, **(1998)**, pp. 2054-2060.

[19] Z. Wang and S. F. Wu, "Helmholtz equation–least-squares method for reconstructing the acoustic pressure field", Journal of the Acoustical Society of America, vol. 102, no. 4, **(1997)**, pp. 2020-2032.

[20] J. Hu and Z. Gao, "Distinction immune genes of hepatitis-induced heptatocellular carcinoma", Bioinformatics, vol. 28, no. 24, **(2012)**, pp. 3191-3194.

[21] J. Yang, B. Chen and J. Zhou, "A Low-Power and Portable Biomedical Device for Respiratory Monitoring with a Stable Power Source", Sensors, vol. 15, no. 8, **(2015)**, pp. 19618-19632.

[22] G. Bao, L. Mi, Y. Geng and K. Pahlavan, "A computer vision based speed estimation technique for localizing the wireless capsule endoscope inside small intestine", 36th Annual International Conference of the IEEE Engineering in Medicine and Biology Society (EMBC), **(2014)**.

[23] X. Song and Y. Geng, "Distributed community detection optimization algorithm for complex networks", Journal of Networks, vol. 9, no. 10, **(2014)**, pp. 2758-2765.

[24] D. Jiang, X. Ying and Y. Han, "Collaborative multi-hop routing in cognitive wireless networks", Wireless Personal Communications, **(2015)**, pp. 1-23.

[25] Z. Lv, A. Halawani and S. Feng, "Multimodal hand and foot gesture interaction for handheld devices", ACM Transactions on Multimedia Computing, Communications, and Applications (TOMM), vol. 11, no. 1s, **(2014)**, pp. 10.

[26] G. Liu, Y. Geng and K. Pahlavan, "Effects of calibration RFID tags on performance of inertial navigation in indoor environment", 2015 International Conference on Computing, Networking and Communications (ICNC), **(2015)**.

[27] J. He, Y. Geng, Y. Wan, S. Li and K. Pahlavan, "A cyber physical test-bed for virtualization of RF access environment for body sensor network", IEEE Sensor Journal, vol. 13, no. 10, **(2013)**, pp. 3826-3836.

[28] W. Huang and Y. Geng, "Identification Method of Attack Path Based on Immune Intrusion Detection", Journal of Networks, vol. 9, no. 4, **(2014)**, pp. 964-971.

[29] X. Li, Z. Lv and J. Hu, "XEarth: A 3D GIS Platform for managing massive city information", Computational Intelligence and Virtual Environments for Measurement Systems and Applications (CIVEMSA), 2015 IEEE International Conference on. IEEE, **(2015)**, pp. 1-6.

[30] J. He, Y. Geng, F. Liu and C. Xu, "CC-KF: Enhanced TOA Performance in Multipath and NLOS Indoor Extreme Environment", IEEE Sensor Journal, vol. 14, no. 11, **(2014)**, pp. 3766-3774.

[31] N. Lu, C. Lu, Z. Yang and Y. Geng, "Modeling Framework for Mining Lifecycle Management", Journal of Networks, vol. 9, no. 3, pp. 719-725, **(2014)**.

[32] Y. Geng and K. Pahlavan, "On the accuracy of rf and image processing based hybrid localization for wireless capsule endoscopy", IEEE Wireless Communications and Networking Conference (WCNC), **(2015)**.

[33] X. Li, Z. Lv and J. Hu, "Traffic management and forecasting system based on 3d gis", Cluster, Cloud and Grid Computing (CCGrid), 2015 15th IEEE/ACM International Symposium on, **(2015)**, pp. 991-998.

[34] S. Zhang and H. Jing "Fast log-Gabor-based nonlocal means image denoising methods", Image Processing (ICIP), 2014 IEEE International Conference on. IEEE, **(2014)**, pp. 2724-2728.

Authors

Yue Xiao, He received his Ph.D. degree in School of Mechanical and Automotive Engineering from Hefei University of Technology in 2014, China. He is currently a lecturer in School of Mechanical and Electrical Engineering, Nanchang Institute of Technology. His research interest is mainly in the area of Vibration and Noise Control, Acoustic Design, Sound Quality. He has published several research papers in scholarly journals in the above research areas.

Mouyou Lin, He received his B.S. degree in School of Mechanical Engineering from Changsha University of Science and Technology in 1990, China. He is currently an associate professor in School of Mechanical and Electrical Engineering, Nanchang Institute of Technology. His research interest is mainly in the area of Automobile Application Engineering and Vehicle Operation Engineering. He has published several research papers in scholarly journals in the above research areas.

Zhenxi Wang, He received his Ph.D. degree in 2011 from Zhejiang University in Hangzhou, China. He is currently an associate professor in School of Science, Nanchang Institute of Technology. His research interest is mainly in the area of Mechanical System Dynamics and Chemical Machinery. He has published several research papers in scholarly journals in the above research areas.